

## Article

# Global Urbanization and Habitat Quality: Interactive Coercive Relationships

Weisong Li <sup>1,2,3</sup> , Jiahui Wu <sup>4</sup>, Yanghaoyue Yuan <sup>4</sup>, Binqiao Duan <sup>4</sup>, Sipei Pan <sup>5,\*</sup> , Wanxu Chen <sup>4,\*</sup>  and Yan Chen <sup>6</sup>

- <sup>1</sup> Experimental Teaching Centre, Hubei University of Economics, Wuhan 430074, China; lws@hbue.edu.cn  
<sup>2</sup> Hubei Key Laboratory of Digital Finance Innovation, Hubei University of Economics, Wuhan 430205, China  
<sup>3</sup> Collaborative Innovation Center for Emissions Trading System Co-Constructed by the Province and Ministry, Wuhan 430205, China  
<sup>4</sup> Hubei Key Laboratory of Regional Ecology and Environmental Change, School of Geography and Information Engineering, China University of Geosciences, Wuhan 430074, China; wjh0726@cug.edu.cn (J.W.); yuan.y.h.y@cug.edu.cn (Y.Y.); duanbq@cug.edu.cn (B.D.)  
<sup>5</sup> College of Land Management, Nanjing Agricultural University, Nanjing 210095, China  
<sup>6</sup> School of Computer Science, China University of Geosciences, Wuhan 430074, China; 20221002134@cug.edu.cn  
\* Correspondence: pamsp@cug.edu.cn (S.P.); cugcwxc@cug.edu.cn (W.C.)

**Abstract:** Urbanization is inevitably accompanied by drastic changes in regional land use and therefore presents an evident influence on ecosystems. Habitat quality (HQ) reflects the ability of a habitat to provide suitable conditions for the survival of an individual or population, and clarifying the interrelationships between urbanization level (UL) and HQ provides insights into sustainable urbanization and ecosystems conservation. Much attention has focused on how urbanization related to HQ at multi-scales, but few studies have analyzed the interactive coercive relationships between UL and HQ on the global county level. To address this gap, we adopted the bivariate spatial autocorrelation and coupling coordination degree (CCD) model to determine their interactive coercive relationships at the county level globally. Results showed that the global average UL was 0.0807, 0.0838, and 0.0857 in 2000, 2010, and 2020, respectively, with a continuously increasing trend. The global average HQ was 0.6186, 0.6133, and 0.6111 for 2000, 2010, and 2020, reflecting opposite declining trends. The Moran's *I* of population urbanization and HQ in 2000, 2010, and 2020 globally remained negative but showed an increasing trend, with values of  $-0.189$ ,  $-0.228$ , and  $-0.254$ , respectively, while those of economic urbanization and HQ and land urbanization and HQ also remained negative and exhibited a similar increasing trend. The spatial autocorrelations for UL and HQ in different dimensions indicated that deserts and plateaus functioned as catchment areas with low UL and HQ. The CCD between UL and HQ in each county globally ranged from 0 to 0.70, while CCD between land urbanization and HQ was the most optimal at 0–0.90. The CCD between population urbanization and HQ was similar to that of economic urbanization in terms of spatial distribution. Nevertheless, the CCD of land urbanization in HQ exhibited the greatest degree of coordination among the three urbanization dimensions during the study period. These findings provided important support for sustainable urbanization and ecosystem protection globally.

**Keywords:** urbanization; habitat quality; bivariate spatial autocorrelation; coupling coordination model; global scale



**Citation:** Li, W.; Wu, J.; Yuan, Y.; Duan, B.; Pan, S.; Chen, W.; Chen, Y. Global Urbanization and Habitat Quality: Interactive Coercive Relationships. *Land* **2024**, *13*, 1943. <https://doi.org/10.3390/land13111943>

Academic Editor: Jianjun Zhang

Received: 5 October 2024

Revised: 31 October 2024

Accepted: 13 November 2024

Published: 18 November 2024



**Copyright:** © 2024 by the authors. Licensee MDPI, Basel, Switzerland. This article is an open access article distributed under the terms and conditions of the Creative Commons Attribution (CC BY) license (<https://creativecommons.org/licenses/by/4.0/>).

## 1. Introduction

Given the challenges posed by global climate change, urbanization presents a major challenge to achieving sustainable development [1,2]. Urbanization inevitably leads to drastic changes in land use, which have profound implications for ecosystems, particularly in terms of habitat quality (HQ) [3]. More than 80% of the regional natural habitat has been lost due to rapid urban expansion [4–6]. Indeed, HQ and urbanization are interrelated [7].

Urbanization exerts considerable strain on natural ecosystems, leading to HQ deterioration. Nevertheless, the processes of urbanization are constrained by ecological degradation and resource scarcity [8]. Moreover, ecological improvement, ecosystem enhancement, and HQ optimization can increase the regional resilience and livability [3]. Therefore, to effectively guide urban planning toward sustainable development, it is essential to examine the interactive coercive relationships between urbanization level (UL) and HQ.

HQ is a key indicator of ecological health [3]. Initially, research on HQ primarily concentrated on its measurement, relying predominantly on data gathered from field surveys [9–11]. However, this method is time-consuming and labor-intensive [12], which makes it challenging to conduct research on a global scale. As technology has advanced, additional methods have been proposed and applied to the quantitative assessment of HQ and analysis of its spatiotemporal evolution [13]. These methods can be classified into two main categories according to their research objectives. The first type of methods primarily focuses on exploring the extensive range of impacts that human activities have on HQ from the multidimensional perspective of economic development [14]. The second type of methods focuses on applying advanced spatial analytical tools and technological means to assess the dynamic changes of HQ and their spatial distribution characteristics across different time scales [15]. Such methods enable the conduct of extensive long-term time series research. In addition, the current field of research continues to deepen and advance, with a specific emphasis on examining the various factors that drive changes in HQ [16,17]. Of particular concern is the acceleration of the globalization process, which has led to an unprecedentedly rapid trend of urban expansion on a global scale. This phenomenon has not only reshaped the geomorphological landscape of the Earth but has also profoundly altered the ecological, economic, and social structures of human societies. Consequently, the changes in HQ and their extensive and far-reaching impacts have emerged as the hottest topics and focal points of exploration in the scientific research community. Indeed, the evolution of HQ and its consequences are now at the forefront of scientific inquiry, attracting significant attention and research efforts [3,18]. By delving into these changes, researchers aim to better understand and address the intricate interplay between human activities and ecological health.

Urban development, as an important engine for social progress and economic prosperity, is undoubtedly a powerful driver of crucial changes in regional HQ [3,18]. The dramatic changes in land-use types during the urbanization process have undoubtedly had far-reaching and multidimensional significant effects on HQ [3,19]. Hence, exploring ways to minimize the negative impacts of rapidly rising levels of urbanization on HQ has emerged as a major challenge for sustainable urban development [20]. Previous research has extensively explored the impacts of UL on the eco-environment [21,22]. These studies have conducted in-depth and extensive analyses focusing on several core aspects: the non-linear negative relationship [23], impacts of changing landscape patterns attributable to UL on HQ [24,25], and simulation of HQ changes [26]. Specifically, Zhu et al. (2020) revealed a nonlinear and negative relationship between HQ and UL [23]. Hu et al. (2022) found that landscape pattern effects on HQ varied in both extent and intensity in the context of urbanization [24]. Luan et al. (2023) predicted that HQ would continue to decline over the next decade [26].

Although numerous attempts have been made at multiple scales from diverse perspectives using different methodologies, the existing research still harbors several flaws. First, in terms of the scale of research, previous studies have tended to focus on the impact of UL on HQ of local regions at a small scale [27], such as metropolitan areas and individual cities [18,23,25,26,28], but few study has attempted to perform such an analysis at the global scale. Moreover, few study has analyzed UL and HQ from the global scale at the county level, even though county-level studies can better detect regional differences [29]. Additionally, the existing studies are confined to examining the unilateral impact of UL on HQ [18,23,25–28], neglecting the mutual interaction between them [7]. Urbanization indeed results in habitat destruction [18]. Yet simultaneously, habitat loss and HQ de-

cline pose grave threats to the sustainability of urban development [8]. In addition, the relationship between urbanization system and HQ is not mutually antagonistic but interdependent and has a symbiotic coupling relationship. The rapid growth of urbanization has a significant role in promoting or damaging the quality of habitats. The improvement of HQ also provides a basic guarantee for the sustainable development of urbanization. Therefore, an in-depth study of the interactive coercive relationship is particularly necessary. Furthermore, most previous studies have primarily focused on a single dimension of urbanization. However, urbanization encompasses more than just an increase in urban population growth [30,31]. It is also accompanied by urban land expansion, rapid economic development, and continuous social progress [32,33]. These four aspects are interconnected and complementary, collectively reflecting the overall UL [32]. Thus, a comprehensive consideration of the impacts of these aspects on urbanization can better reflect the essence of UL [29]. Focusing on the interactive coercive relationships between different dimensions of UL and HQ can make a better multi-perspective view for ecological conservation and sustainable urban development.

To compensate for the research gaps mentioned above, this study introduced the bivariate spatial autocorrelation and coupling coordination degree (CCD) model to reveal the interactive coercive relationships between UL and HQ at the county level globally. The goals of this study were (1) to analyze the spatiotemporal patterns of global UL and HQ, (2) to reveal the bivariate autocorrelation between UL and HQ, and (3) to assess the CCD between global UL and HQ.

## 2. Materials and Methods

### 2.1. Data Sources and Processing

In assessing global HQ indicators using the InVEST (Integrated Valuation of Ecosystem Services and Tradeoffs) model, the core data requirements cover both land-use and road information. Our study relied heavily on the European Space Agency’s Climate Change Initiative Land Cover database (<https://www.esa-landcover-cci.org/>, accessed on 13 September 2024) as the main source of land-use data. This dataset provided detailed land cover classes, satellite-observation-based, 300 m spatial resolution, and a global coverage making it a key foundation for the assessment of HQ (Table 1). Road data and vector data to calculate threat factors for HQ were obtained from the Global Roads Open Access Data Set dataset maintained by the Socioeconomic Data and Applications Center (<https://sedac.ciesin.columbia.edu/>, accessed on 13 September 2024). These datasets provided the spatial resolution and global coverage necessary to accurately model HQ globally, accounting for the varying influence of land use and road presence on habitat degradation and fragmentation. In addition, the population density data were derived from LandScan (<https://landscan.ornl.gov/>, accessed on 13 September 2024) at a resolution of 1000 m. The global gross domestic product at 1000 m precision gridding was obtained from Chen et al. (2022) [34].

**Table 1.** Data description.

| Data Types                          | Data Sources and Description   | Preprocessing Instructions   |
|-------------------------------------|--|--|
| Land-use and land-cover change data | European Space Agency’s Climate Change Initiative Land Cover database ( <a href="https://www.esa-landcover-cci.org/">https://www.esa-landcover-cci.org/</a> ). The data spatial resolution is 300 × 300 m. | Extracted using ArcGIS 10.3 Arc Toolbox/Spatial Analyst Tools/Reclass/Reclassify<br>Extracted using ArcGIS 10.3 Arc Toolbox/Spatial Analyst Tools/Extract/Extract by Attributes<br>Extracted using ArcGIS 10.3 Arc Toolbox/Spatial Analyst Tools/Zonal/Zonal Statistics tool |
| Road data                           | The Socioeconomic Data and Applications Center ( <a href="https://sedac.ciesin.columbia.edu/">https://sedac.ciesin.columbia.edu/</a> )   |  |
| Population density data             | LandScan ( <a href="https://landscan.ornl.gov/">https://landscan.ornl.gov/</a> ). The data spatial resolution is 1000 × 1000 m.  | Extracted using ArcGIS 10.3 Arc Toolbox/Spatial Analyst Tools/Zonal/Zonal Statistics tool  |
| GDP data                            | The global gross domestic product at 1000 m precision gridding was obtained from Chen et al. (2022) [34].  | Extracted using ArcGIS 10.3 Arc Toolbox/Spatial Analyst Tools/Zonal/Zonal Statistics tool  |

## 2.2. UL Measurement

Population growth is the core of population urbanization, economic growth drives economic urbanization, while land-use intensity is the characteristic of land urbanization [35–37]. The interrelationships among changes in population, economic growth, and land-use intensity are complex and mutually reinforcing, collectively contributing to a comprehensive understanding of urbanization. Due to the challenges associated with quantifying and spatializing social urbanization, this aspect was excluded from the present study. Compared to previous studies, this study selected population density, economic density, and land-use intensity to characterize population urbanization, economic urbanization, and land urbanization, respectively. Land-use intensity was calculated according to Peng et al. (2023) [38]. Following the standardization of these three indicators, the global UL was derived through an equal-weighting calculation.

## 2.3. HQ Assessment

This study was an in-depth application of the HQ Module of the InVEST model, aiming to provide a comprehensive and accurate assessment of HQ within a given region [18,39]. Notably, the InVEST model used in this study, was designed to be universally applicable. This module evaluated HQ and degradation by analyzing various land-cover types alongside their corresponding threat factors. First, we prepared land-cover maps and compiled data on significant threat factors. Urban sprawl and agricultural expansion were identified as major threat factors that considerably influence HQ.

Then, for each category of land cover and the associated threat factor, we set parameters including suitability, relative impact, and weight [40–42]. Habitat suitability ( $H_x$ ), quantified on a range from 0 to 1, serves as an indicator of the potential quality of a habitat. The relative impact ( $r_i$ ) and weight ( $W_i$ ) of each threat factor indicate the relative importance of each threat factor to HQ. We then entered the land-cover map and threat factor data into InVEST to execute and parameterize the HQ module. The model first calculated the habitat degradation value ( $D_{xj}$ ) for each pixel using the following equation:

$$D_{xj} = \sum_{i=1}^n \left( \frac{r_i \cdot I_i(x) \cdot W_i}{1 + k \cdot d_{ix}^2} \right) \quad (1)$$

where  $I_{i(x)}$  represents the influence degree of the threat factor  $i$  on pixel  $x$ ,  $d_{ix}$  denotes the distance from the source of threat factor  $i$  to pixel  $x$ , and  $k$  serves as a correction parameter used to adjust the range attenuation function. Following the determination of the degradation value for each pixel, the model calculates the HQ value ( $Q_x$ ) of each pixel using the equation provided below:

$$Q_x = \frac{H_x \cdot (1 - D_{xj})}{H_x + D_{xj}} \quad (2)$$

Finally, the model generates values about HQ and degradation for each pixel. We evaluated the condition of HQ through both visual and statistical analysis of the results. The findings of this assessment would provide a scientific foundation for the formulation of ecological conservation and management strategies as well as for the identification of critical areas for habitat protection aimed at mitigating threats and enhancing overall ecological health.



#### 2.4. Bivariate Spatial Autocorrelation

Spatial autocorrelation reflects the degree to which the values of a geographic phenomenon or attribute in one region are correlated with those in neighboring regions [35]. In this study, we described the spatial clustering characteristics (spatial positive correlation) and spatial dispersion (spatial negative correlation) between UL and HQ using bivariate Moran's  $I$  [43,44]. The global bivariate Moran's  $I$  was used to assess whether spatial correlation existed and to what degree, while the local bivariate Moran's  $I$  was used to evaluate the presence of spatial correlation in specific areas. The equations for the calculations were as follows:

$$\text{Moran's } I = \frac{n \sum_{i=1}^n \sum_{j \neq i}^n w_{ij} \overline{UL}_i^e \overline{HQ}_j^u}{(n-1) \sum_{i=1}^n \sum_{i \neq j}^n w_{ij}} \quad (3)$$

$$\text{Moran's } I = \overline{UL}_i^e \sum_{j=1}^n w_{ij} \overline{HQ}_j^u \quad (4)$$

where  $\overline{UL}_i^e$  and  $\overline{HQ}_j^u$  are the standardized UL and HQ of the  $i$ -th and  $j$ -th unit, respectively, and  $w_{ij}$  is an  $n \times n$  spatial weight matrix.  $n$  is the number of units.

#### 2.5. CCD Model

In this study, the interactive coercive relationship between UL and HQ was investigated using CCD [45,46]. Previous studies showed that a complex non-linear coupling relationship existed between UL and HQ systems, and CCD can well reveal the degree and the evolutionary trend of the coupling between them [3]. The coupling degree ( $C$ ) can be used to a certain extent to assess the strength of the coupling between two systems, but errors in assessment may arise when relying solely on the coupling degree, particularly in cases where the two subsystems exhibit similar and low values. Calculating the coupling degree alone can lead to erroneous evaluation results with a high degree of synergistic development. Consequently, a coupled coordination model ( $D$ ) was also constructed, as follows:

$$C = \left\{ \overline{HQ} \cdot \overline{UL} / [(\overline{UL} + \overline{HQ}) / 2]^2 \right\}^{1/2} \quad (5)$$

$$T = \alpha \overline{UL} + \beta \overline{HQ} \quad (6)$$

$$D = \sqrt{C \cdot T} \quad (7)$$

where  $\alpha$  and  $\beta$  are undetermined coefficients set to 0.5, respectively, and  $\alpha + \beta = 1$ .  $T$  represents the comprehensive coordination index. Generally, CCD results are categorized into four stages.  $0 < D \leq 0.2$  indicates extreme incoordination;  $0.2 < D \leq 0.4$  indicates moderate incoordination;  $0.4 < D \leq 0.6$  indicates basic coordination;  $0.6 < D \leq 0.8$  indicates moderate coordination;  $0.8 < D \leq 1$  indicates high coordination.

### 3. Results

#### 3.1. Spatiotemporal Patterns of Global UL

The global average UL at the county level in 2000, 2010, and 2020 was 0.0807, 0.0838, and 0.0857, respectively, indicating a continuous growth trend (Figure 1b). Among all the 312,432 counties globally, the percentages of counties with various UL ranges remained relatively stable during the research period, with the largest percentage belonging to those with UL below 0.05, but this showed a definite downward trend from 46.06% in 2000 to 44.26% in 2020 (Figure 1c). Counties with UL values between (0.05, 0.10] and (0.10, 0.20] had similar percentages, and all of them showed an increasing, but then decreasing trend (Figure 2a,c). Although counties with UL values between (0.20, 0.30] and (0.30, 0.90] were fewer in number, all showed an increasing trend. It is worth noting that counties with UL between 0.30 and 0.90 almost doubled in the two decades, from 1.09% in 2000

to 1.99% in 2020 (Figure 2c), indicating that counties around the world experienced an extremely rapid urbanization process in the past two decades (Figure 2a,c). Spatially, UL distribution showed distinctive regional differences (Figure 2). High-UL counties were mainly concentrated in eastern and southern Asia, eastern Europe, central and sub-Saharan Africa, southeastern South America, and southern North America, mainly because of the relatively dense populations and high urbanization rates in these regions. The overall distribution pattern showed limited changes throughout the study period. The addition of counties with UL values between 0.30 and 0.90 was concentrated in the regions mentioned above, indicating that these regions would remain the most dominant areas for urbanization and development.

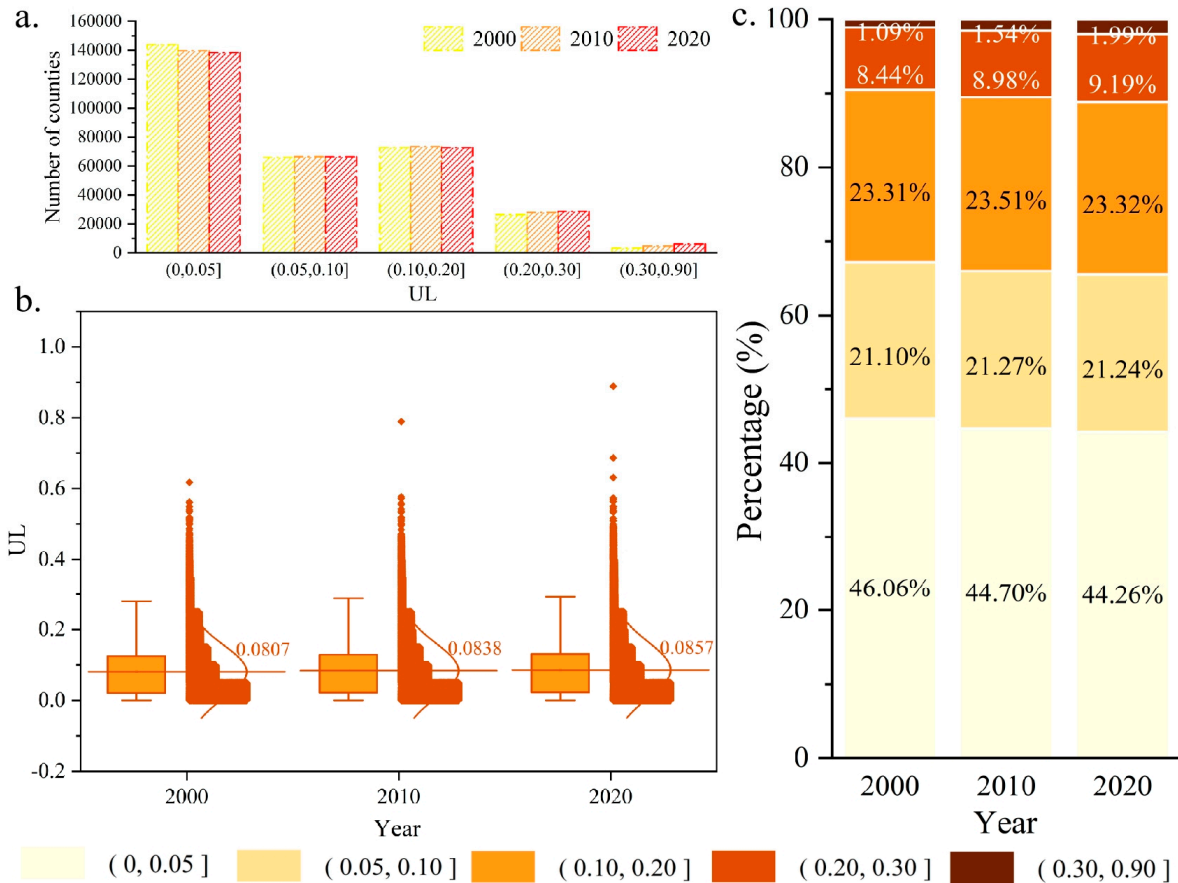


**Figure 1.** Changes in global UL from 2000 to 2020. (a) Comparison of the number of counties with different UL; (b) boxplot of the distribution of UL by county; (c) percentage of counties with different UL.

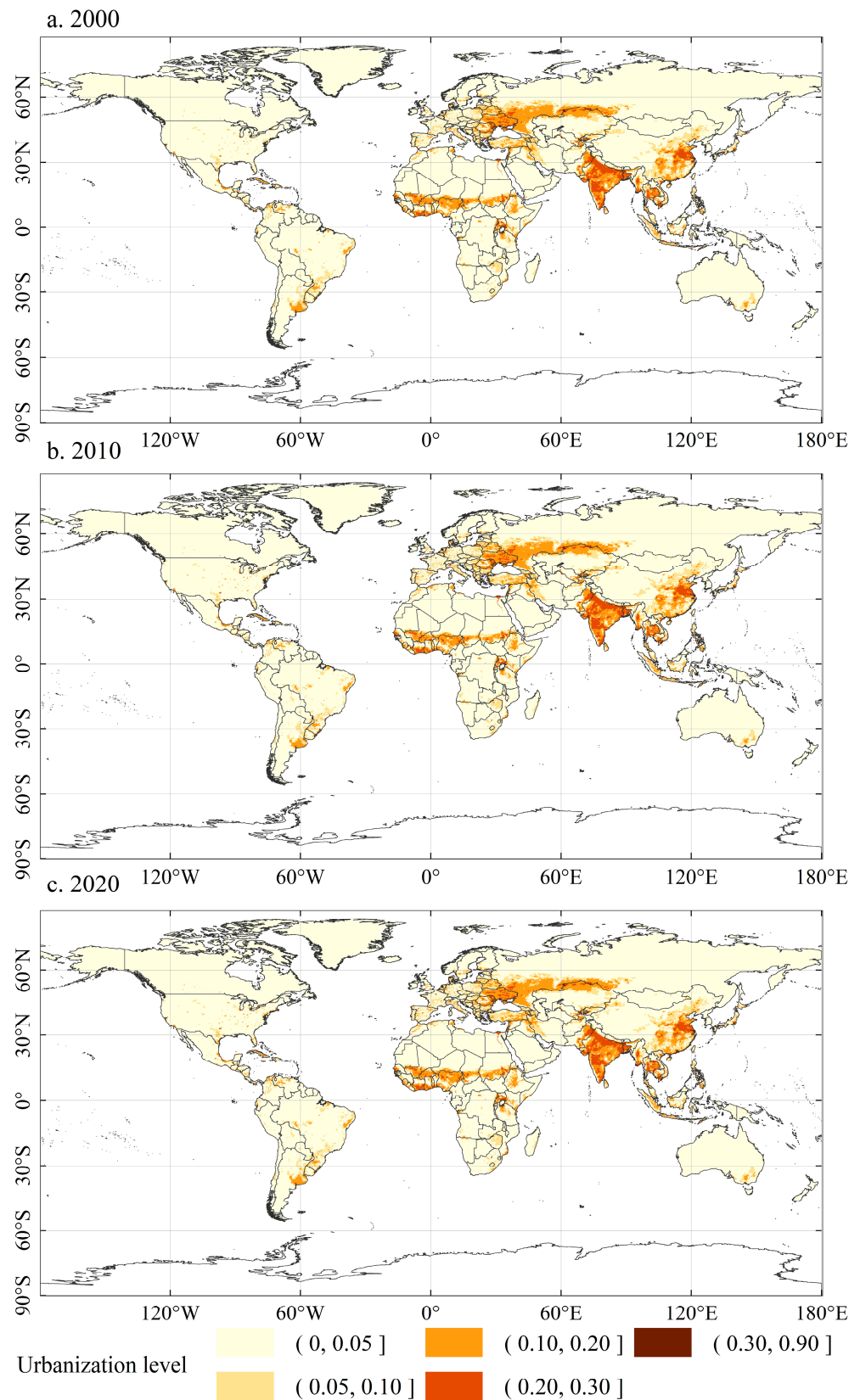


**Figure 2.** Spatial distribution pattern of global UL from 2000 to 2020.

### 3.2. Spatiotemporal Patterns of Global HQ

The global average HQ at the county level in 2000, 2010, and 2020 was 0.6186, 0.6133, and 0.6111 (Figure 3b), respectively, indicating a continuous downward trend, exhibiting

the opposite trend compared that of UL. Among all the 312,432 counties globally, the percentages of counties with various HQ ranges remained relatively stable through the study period. The largest percentage belonged to counties with an HQ between 0.35 and 0.5, but these showed a slight downward trend, from 34.18% in 2000 to 33.3% in 2020 (Figure 3c). However, the percentage of counties with HQ between 0 and 0.35 showed an increase, from 4.72% in 2000 to 6.63% in 2020 (Figure 3c). The percentage of counties with a better HQ of more than 0.7 showed a downward trend similar to that of those with values from 0.35 to 0.5 (Figure 3a,c). The spatiotemporal distribution of global HQ also exhibited distinct regional differences (Figure 4). High-HQ counties were mainly concentrated in eastern and southern Asia, northern and western Europe, southern Africa, and most regions of the American continent. Although the overall distribution pattern did not change much, there was a clear downward trend of HQ in localized areas, most notably in the Amazon River Basin in South America and the Congo Basin in Africa, suggesting that the ecosystems of these two major tropical rainforests have suffered extremely severe damage due to anthropogenic causes.

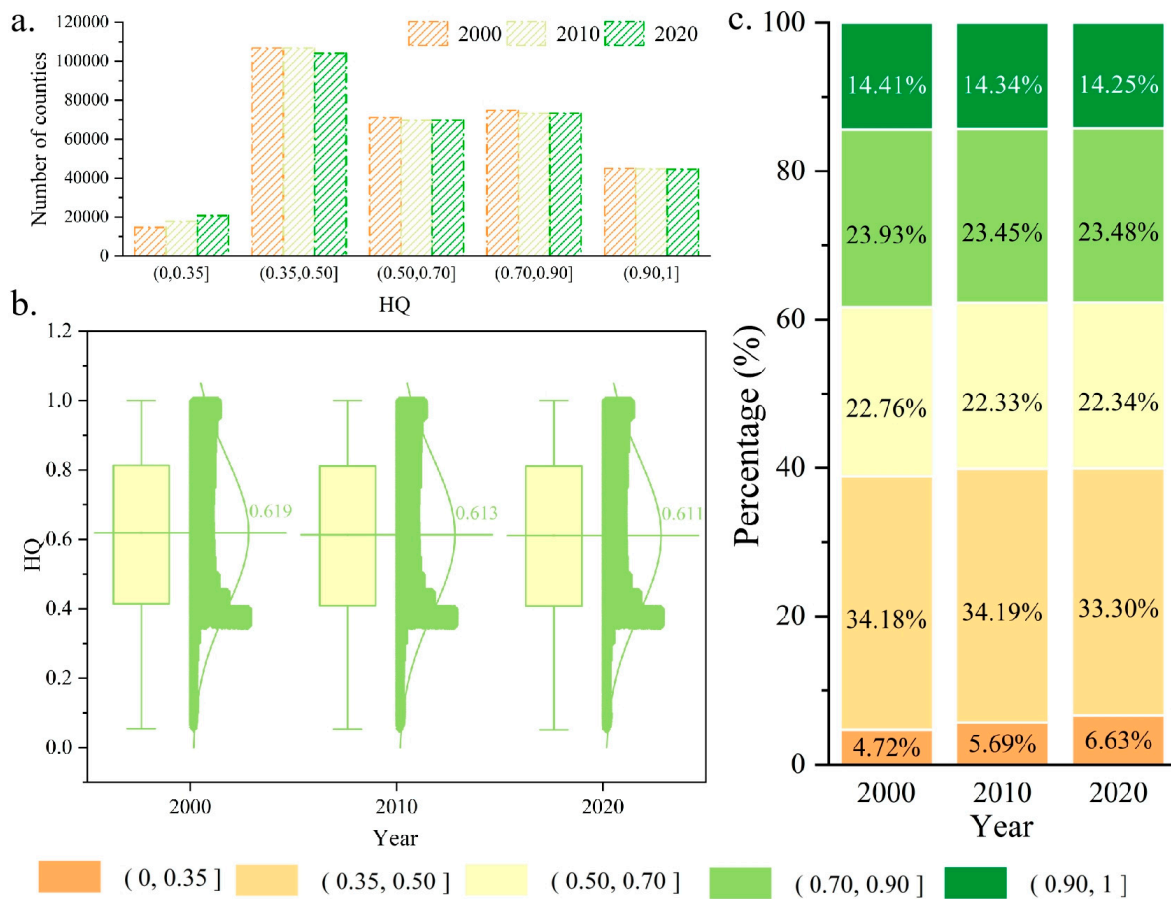


**Figure 3.** Changes in global HQ from 2000 to 2020. (a) Comparison of the number of counties with different HQ; (b) boxplot of the distribution of HQ by county; (c) percentage of counties with different HQ.

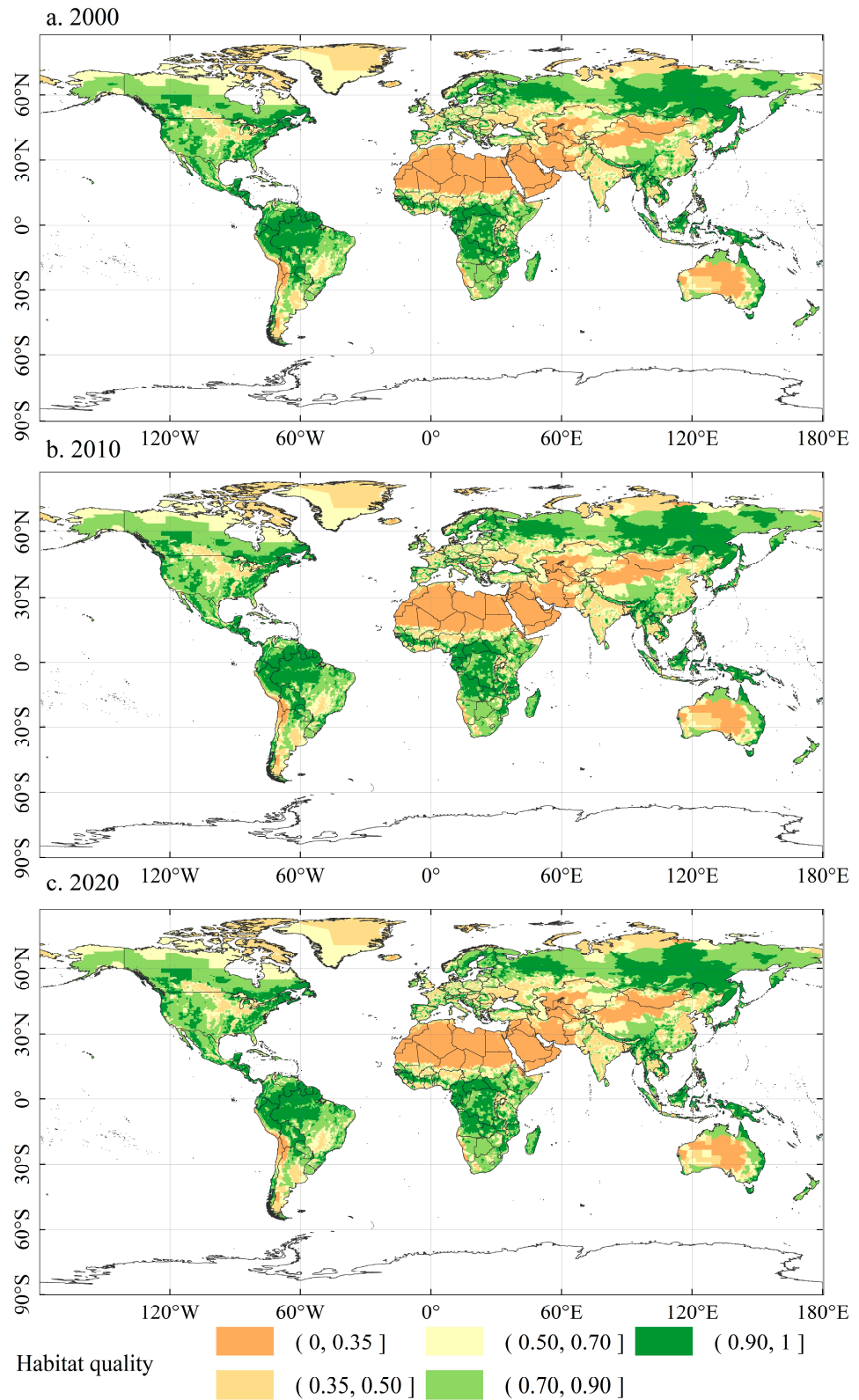


**Figure 4.** Spatiotemporal distribution of global HQ from 2000 to 2020.

### 3.3. Bivariate Autocorrelation Between UL and HQ

The results showed that Moran’s *I* of population urbanization and HQ in 2000, 2010, and 2020 globally remained negative but showed an increasing trend, which was  $-0.189$ ,  $-0.228$ , and  $-0.254$ , respectively. At the county scale, the proportion of the non-significant type was the largest, accounting for almost half of the counties, and showed an increasing



trend over time, increasing to 45.99% in 2020 (Figure 5). The low-high type was the second most prevalent type, followed by the low-low type, with a decreasing trend. The high-high type was the least common, accounting for only 0.91% of the types by 2020, and also showed a decreasing trend (Figure 5). The spatial distribution pattern did not change much through the years (Figure S1). The low-high type was widespread across the continents, being most common on the American continent and in southern Africa and the whole of Russia. The low-low type was most concentrated in desert areas, such as the Sahara Desert in Africa, the Taklimakan Desert in China, and the Great Victoria Desert in Australia. The non-significant type always appeared around the low-low type, a feature that occurred similarly around the globe. It is worth mentioning that the North China Plain and Sichuan Basin in China and the Gangetic Plain in India, where the population was dense, were the main areas where the high-low type was concentrated. Only a very small number of counties in the Congo River Basin exhibited the high-high type.

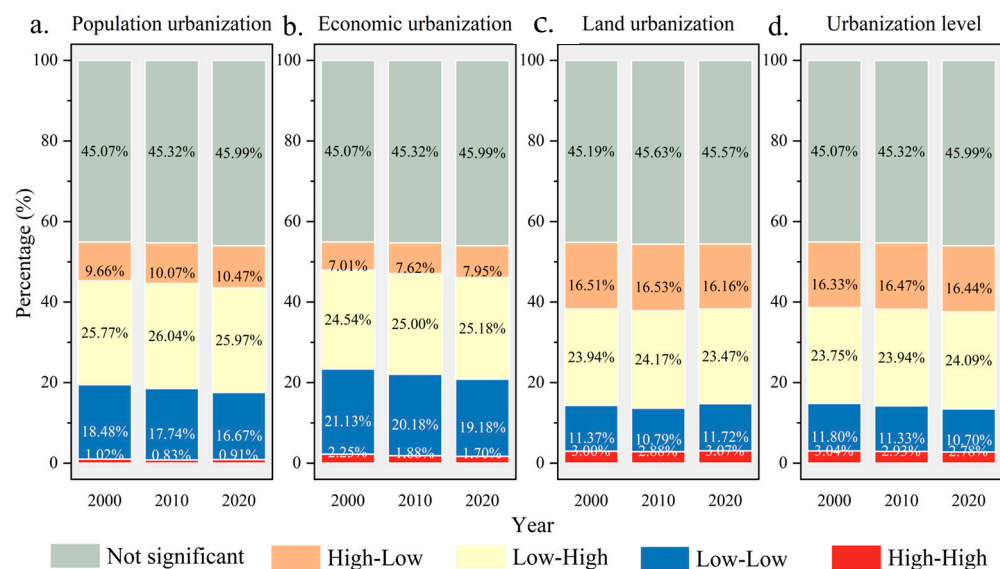


**Figure 5.** Percentage of different spatial aggregation types.

The results of the spatial autocorrelation between economic urbanization and HQ showed that Moran's  $I$  was negative and increasing globally in 2000, 2010, and 2020 at  $-0.220$ ,  $-0.221$ , and  $-0.241$ , respectively. The non-significant type had the largest proportion over time, almost half ( $>45\%$ ), followed by the low-high and low-low types (Figure 5). The smallest share was the high-high type, which had a downward trend, accounting for only 1.70% of the total by 2020 (Figure 5). The spatial autocorrelation distribution pattern of economic urbanization and HQ was quite similar to that of population urbanization and HQ (Figure S2). It is worth noting that the high-high type, with the lowest percentage, was found in the more economically developed regions of the United States East Coast, central Europe, Japan, and the eastern coast of China.

The results of the spatial autocorrelation between land urbanization and HQ showed that Moran's  $I$  was still negative globally in 2000, 2010, and 2020 with an increasing trend of  $-0.443$ ,  $-0.464$ , and  $-0.481$ , respectively. The non-significant type had the largest share over time, almost half ( $>45\%$ ) (Figure 5). This was closely followed by the two types of low-high and high-low. The smallest share was taken by the high-high type, which showed a downward trend and accounted for only 2.860% of the total by 2020 (Figure 5). The spatial autocorrelation distribution pattern of land urbanization and HQ was quite similar to those of population urbanization and economic urbanization with HQ (Figure S3), except that the high-low type was widely distributed in Asia, Africa, and Europe, mainly in eastern Europe, sub-Saharan Africa, South Asia, and the North China Plain of China. South China was the main concentration area of the high-high type.

Overall, Moran's  $I$  of UL and HQ in 2000, 2010, and 2020 globally remained negative and showed an increasing trend, which was  $-0.447$ ,  $-0.468$ , and  $-0.486$ , respectively. The non-significant type had the largest share over time, almost half ( $>45\%$ ), followed by the low-high and high-low types, while the smallest share remained the high-high type, which showed a downward trend, accounting for only 2.78% of the total by 2020 (Figure 5). The spatial autocorrelation types of UL and HQ were quite analogous to those of land urbanization and HQ in number and also showed extremely similar distribution characteristics, with little difference in spatial distribution (Figure 6).

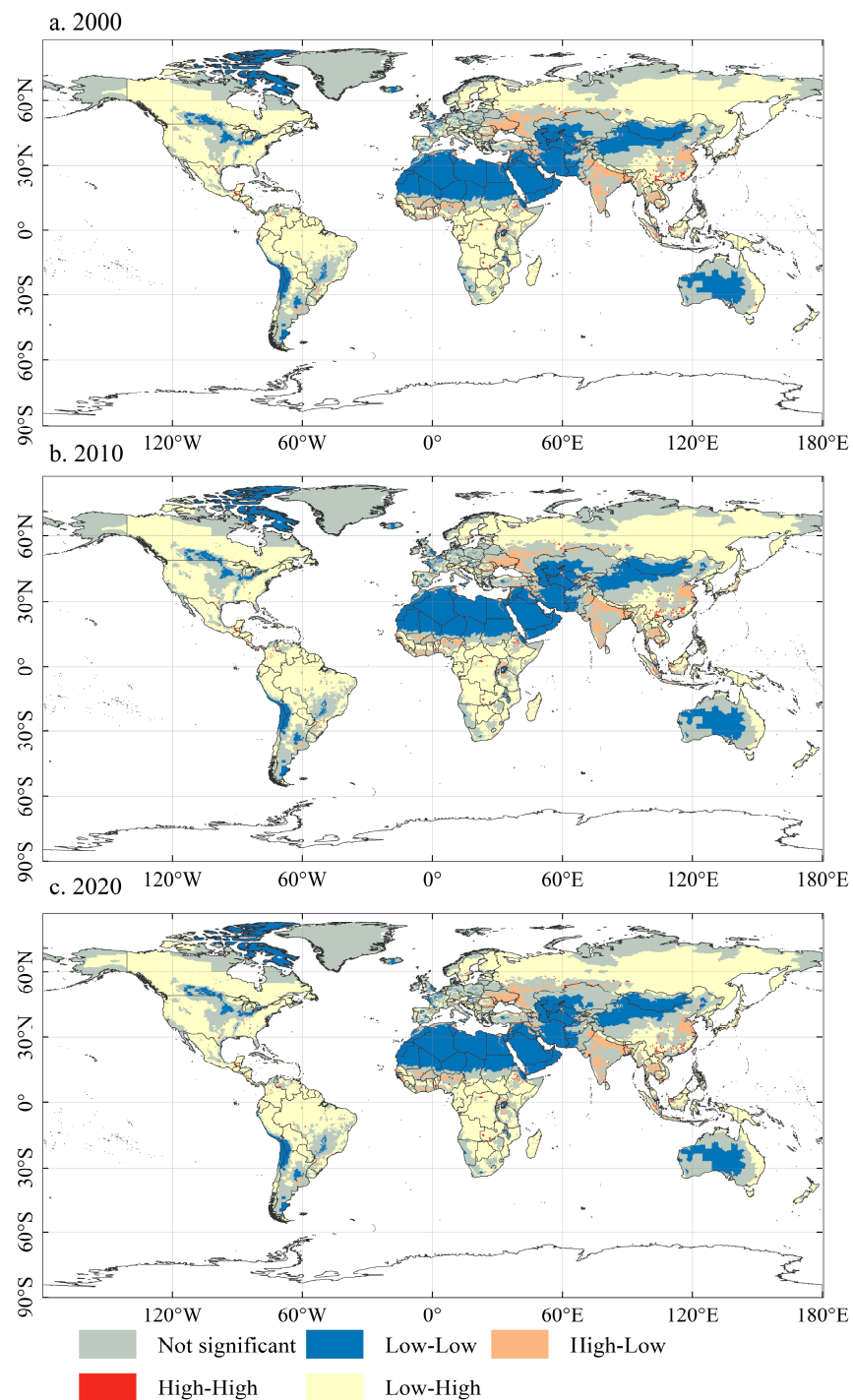


**Figure 6.** Bivariate LISA cluster maps between global UL and HQ from 2000 to 2020.

### 3.4. CCD Between Global UL and HQ

The CCD between population urbanization and HQ at the global county scale ranged from 0 to 0.85. More than half of the counties had a CCD that was in extreme incoordination and trended downward over the study period (Figure 7). The spatial distribution revealed some regional differences, but the variation through the years was not significant (Figure S4). Counties with low CCD were widespread across all continents, whereas regions with high CCD were concentrated in densely populated areas in eastern and southern Asia, such as the eastern coast of China, the Gangetic Plain of India, and some South Asian countries. Counties with relatively high CCD were sporadically located in Europe, the southern part of North America, and southern Africa.

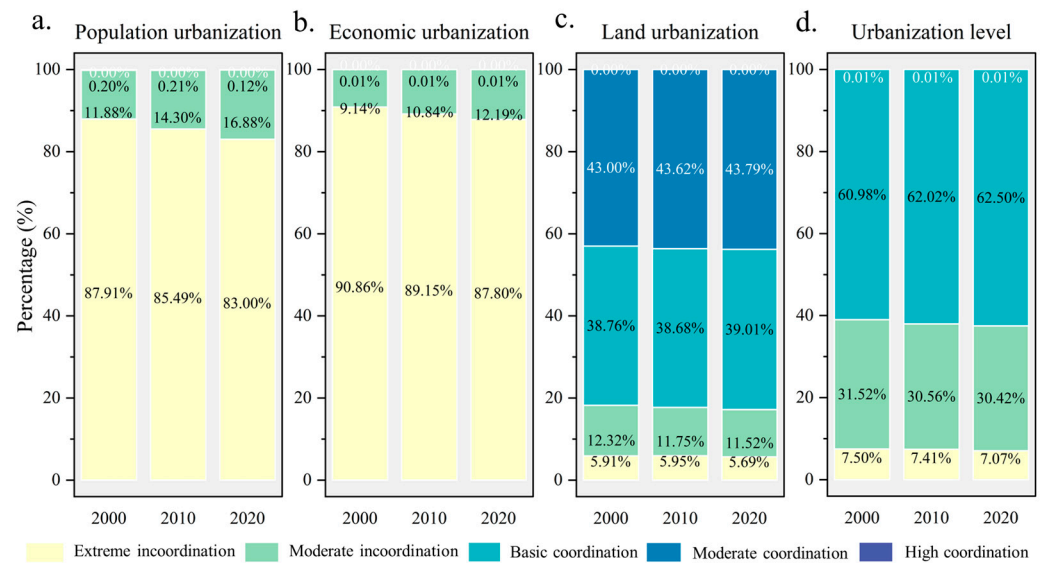


**Figure 7.** Percentage of different coupling coordination degree types.

In the case of economic urbanization and HQ, the CCD ranged from 0 to 0.80, with most cases being in a state of extreme and moderate incoordination. The overwhelming majority of the counties had a CCD lower than 0.2. This percentage reached more than 90% (90.86%) in 2000, but then trended downward, falling to 87.8% in 2020 (Figure 7). Only a very small number of counties had a CCD greater than 0.3. Although this proportion increased, the increase was very limited, especially for counties with a CCD greater than 0.5, which accounted for only 0.01% of the total in 2020 (Figure 7). Counties with high CCD were mainly concentrated in economically developed and densely populated regions, especially the eastern coast of the United States in North America, developed countries in Europe, the eastern coast of Japan and China in East Asia, and southern India and New Zealand in Oceania, similar to the spatial distribution pattern of population urbanization and HQ (Figure S5). It is worth noting that there was a significant expansion through time of high CCD counties in Asia, particularly in China, India, and most of South Asia, indicating that these countries experienced extremely rapid economic development over the past two decades. High CCD counties were largely absent in African countries, suggesting that economic development there has been extremely limited.

The CCD between land urbanization and HQ varies between 0 and 0.90. The CCD of land urbanization and HQ in most counties globally was in basic and moderate coordination. The majority of the counties had a CCD of more than 0.5, showing an overall growth trend. Moreover, counties with various CCD were relatively evenly represented in terms of number (Figure 7). Spatially, counties with high CCD were mainly located in eastern Asia (e.g., China and Japan) and southern Asia (e.g., India, Thailand, and Malaysia), sub-Saharan Africa, eastern Europe, southern North America (e.g., United States and Mexico), eastern South America (e.g., Brazil and Argentina), and southeastern Oceania (e.g.,

southeast Australia and New Zealand) (Figure S6). Areas with counties with low CCD were concentrated in deserts, plateaus, and cold regions of the Arctic Circle.

Overall, the CCD at the global county scale ranged from 0 to 0.70. In addition, more than half of the counties globally have achieved basic coordination, with an increasing trend over the study period (Figure 7). Counties with CCD greater than 0.2 were widely distributed across the seven continents, with the highest concentrations in southern Asia, sub-Saharan Africa, eastern Europe, and eastern South America (Figure 8). Sparsely populated desert areas and cold regions continued to be the main concentrations of counties with low CCD.

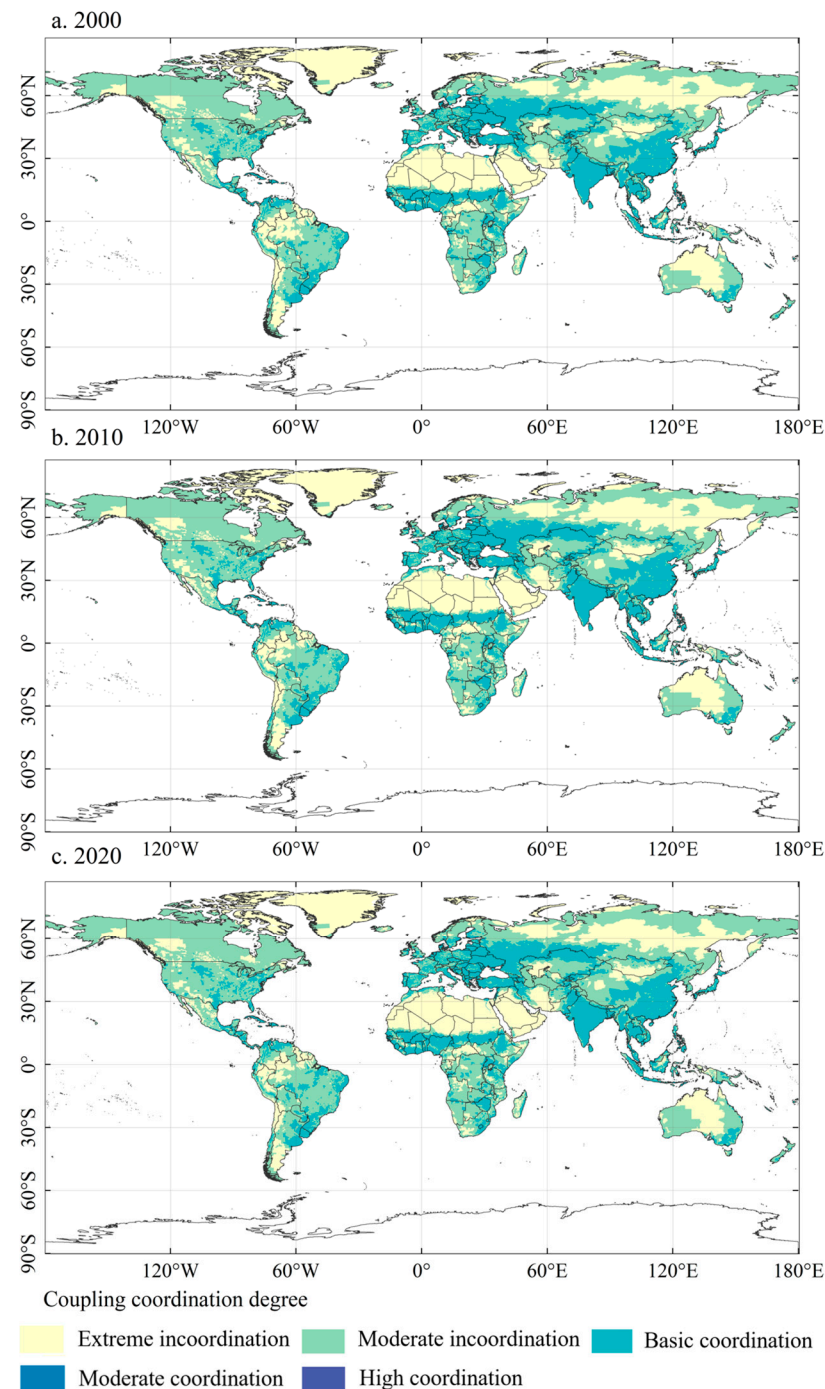


**Figure 8.** Spatiotemporal distribution of CCD between global UL and HQ from 2000 to 2020.



## 4. Discussion

### 4.1. Interpretation of Findings

Urbanization is an inevitable trend in socioeconomic development [29], and urban areas are forecasted to continue expanding in the future [47]. This expansion could have a serious impact on natural habitat [48]. This highlights the urgency of revealing the interactive coercive relationships between UL and HQ. As revealed by our findings, the global average UL at the county level was 0.0807, 0.0838, and 0.0857 for the years 2000, 2010, and 2020, respectively, indicating a continuous growth trend. Such trends in urban development inevitably put enormous pressure on the environment. Counties with a UL below 0.05 had the highest percentage during the study period. Following Northam's classification of stages of urbanization, a city is considered to be in an accelerated stage of development when its UL is between 0.3 and 0.7 [3]. However, this definition is based on population urbanization and does not consider spatial and socioeconomic aspects. When we strip away other aspects of urbanization, we find that most of the counties with UL below 0.005 also have population urbanization rates between 0.3 and 0.7. This is also an indication that most countries in the world are still in rapid urbanization at this stage. Therefore, the problem of how to achieve green and sustainable urban development in the face of rapid urbanization to mitigate environmental losses has become a very important issue [49]. We also found that high-UL counties were mainly concentrated in eastern and southern Asia, eastern Europe, central and sub-Saharan Africa, southeastern South America, and southern North America. This is mainly a result of the relatively dense populations in these regions. Furthermore, the overall distribution pattern did not change much, indicating that these locations have had a huge gravitational effect through the past 20 years due to their relatively good geographical, economic, social, and cultural development conditions [50,51].

We found that the global average HQ values at the county level were positive in 2000, 2010, and 2020 (0.6186, 0.6133, and 0.6111, respectively), but indicated a continuous downward trend, implying that areas with higher or lower HQ tend to cluster, but with some attenuation. This is unanimously supported by Zhu et al. (2020) [23], who found that Moran's *I* of HQ in Nanjing showed a continuing downward trend. However, according to Zhu et al. (2020) [28], Moran's *I* showed a rising trend in Hangzhou, indicating an improving spatial agglomeration of HQ. This also indicated that some cities can achieve better sustainable development despite the adverse environmental effects of urbanization. We also found that high-HQ counties were mainly concentrated in eastern and southern Asia, northern and western Europe, southern Africa, and most regions of the American continents. These areas, especially the tropical rainforest areas, were usually located in lower latitude zones, so the protection of tropical rainforests is extremely important. Nevertheless, tropical rainforests have suffered the most severe ecological damage [52,53]. As our results revealed, there is a clear downward trend of HQ in the Amazon River Basin and Congo Basin.

Notably, the global average HQ at the county level showed the opposite trend of the UL trend. This indicates to some extent that the urbanization process is likely to lead to the degradation of HQ. Bai et al. (2019) [18] revealed a typical association between landscape change and topography during urbanization, and Zhu et al. (2020) [23] revealed a nonlinear negative relationship between HQ and UL. It has been shown that urban expansion areas in China are important concentration areas with serious habitat degradation, which is especially the case for plain areas and areas with intense human activities, where the HQ has decreased significantly [18]. This outcome is not exclusive to China but is a global characteristic. In the changes in HQ, human activities undoubtedly play a dominant role [54]. Although studies have indicated that the global decline in natural areas is primarily due to the expansion of cropland, urban expansion is considered to be a secondary cause [55,56]. However, urban expansion leads to cropland loss, and indirectly, a reduction in cropland may lead to a reduction in the forest land elsewhere, ultimately leading to HQ degradation [49].



The principle of sustainable development requires that environmental, economic, and social impacts be considered in an integrated manner [57]. A city is a complex entity that promotes population, social, and economic development, the sustainability of which will change and improve urban resilience and livability [58]. However, previous research has focused mainly on the single aspect of population urbanization, the most commonly used indicator of global urbanization prospects [30,31]. However, the four dimensions of society, land, economy, and population are commonly adopted to describe the level of urbanization [29,32,33,59]. As a result, different aspects of urbanization may affect HQ in different ways. For example, we found that more than half of the counties worldwide had a CCD between population urbanization and HQ that was lower than 0.15, at extreme incoordination. In contrast, the majority of the world's counties have a CCD between land urbanization and HQ greater than 0.5, which is a high degree of coordination. There are many places in the world where the rate of land urbanization is much quicker than the rate of population urbanization, leading to serious urban expansion [60], especially among the most populous developed countries. In China, for example, the urbanization rate increased by more than 30% over the past several decades, from 17.92% in 1978 to 58.52% in 2017, while the urban area has expanded significantly from 9775 km<sup>2</sup> to 56,225 km<sup>2</sup> between 1985 and 2017 [61]. This is a nearly fivefold increase. It is noteworthy that the spatial distribution of high CCD between population urbanization and HQ is similar to that of high CCD between economic urbanization and HQ, both being mainly concentrated in densely populated areas in East Asia and South Asia. Studies have found that urban densification can mitigate urban expansion to some extent [49], implying that urban sprawl can be controlled in some regions by reducing the demand for construction land [47] and thereby alleviating environmental pressures [62,63], particularly in densely populated developing countries such as China and India. However, in sparsely populated countries, such as the United States and Australia, this strategy is not effective [64,65].

China has made remarkable achievements in the construction of new-type urbanization, focusing on people-oriented, ecological civilization, and cultural heritage. Particularly in the construction of ecological civilization, China has increased its efforts to protect the ecological environment, promoted green and low-carbon development, and achieved a win-win situation between urbanization and HQ. The research results showed high coupling coordination in eastern China. In the European region, Germany and France have been at the forefront of ecological restoration and green transformation. These countries have made significant progress toward the transformation from industrial wasteland to green ecological zone and are committed to promoting global sustainable development.

#### 4.2. Policy Implications

HQ is a crucial indicator of sustainable urban development. Areas with high HQ were typically found in tropical rainforests, plains, and rivers and lakes that possess favorable ecological conditions. However, regions suitable for urban development were often in proximity to ecologically sound areas [48,66], which means that urbanization inevitably has a negative impact on HQ [67]. Therefore, protecting high HQ areas is particularly important. Future development should not and must not come at the expense of these critical regions. Instead, the previous development model that prioritized economic efficiency over ecological considerations should be abandoned and environmental protection should be regarded as a fundamental aspect of urban development [58]. Ecologically sensitive zones including the Amazon rainforest, the Congo Basin, and the Ganges River Basin require special attention.

Economically developed urban areas were usually have low HQ. The impact of economic urbanization on HQ is two-sided. Globally, most cities have struggled to achieve effective environmental protection amid rapid development, leading to ongoing biodiversity loss and a decline in HQ [21]. However, some cities, particularly in East Asia and Eastern Europe, have recognized the importance of integrating ecological foundations into urban planning and development. These cities have made considerable progress toward

sustainability by exploring their unique development paths. They have promoted socioeconomic development and population agglomeration while simultaneously improving HQ. This indicates that urban development does not necessarily result in environmental degradation. While the urban densification discussed earlier can positively contribute to urban environmental protection in certain areas, it is not universally applicable to all cities [49]. Consequently, the local government must identify strategies to implement sustainable development tailored to their specific contexts, drawing on lessons learned from the past, and integrate the principles of sustainable development into urban policy formulation. As technology advances, an increasing array of tools will be applied to model future urban development and environmental changes. This is undoubtedly a positive development. However, current urban systems often rely on relatively simplistic land-use simulation models [68,69], and the simulation of environmental changes [70], especially HQ in urban development, is insufficiently mature to provide targeted development strategies for cities. Therefore, urban planners must also leverage technological tools to address specific environmental aspects of sustainable urbanization in their planning efforts, ensuring the livability of residents [71].

#### 4.3. Validity and Uncertainty of This Study

This study emphasized the interactive coercive relationships among UL and HQ by analyzing the spatiotemporal dynamic variations and CCD between different urbanization aspects and HQ. Nevertheless, the study had certain limitations. Firstly, due to the limitation of data accuracy, this study only comprehensively evaluated UL from the three aspects of population, economy, and land urbanization, which may be different from other index systems. To obtain more accurate results, more accurate data support is needed. Future research will try to explore other indicators to make up for the shortcomings of the existing evaluation system. Secondly, species diversity is an important indicator of HQ [12,17]. However, in this study, HQ was calculated predominantly based on land-use data by setting parameters in the InVEST model without consideration of the characteristics of different species. Future studies can improve the evaluation of HQ by combining it with species distribution modeling. Lastly, this study only analyzed the interactive coercive relationships between UL and HQ. The mechanisms of the interaction between them remain unknown and thus require further investigation.

## 5. Conclusions

This study provided novel information on the interactive coercive relationships between global UL and HQ. The analysis of different aspects of urbanization to HQ provided insights into the spatiotemporal variation in the development of UL and HQ globally. The results showed that the global average UL values of counties in 2000, 2010, and 2020 were 0.0807, 0.0838, and 0.0857 with a continuous growth trend, while the global average HQ values of counties in 2000, 2010, and 2020 were 0.6186, 0.6133, and 0.6111, exhibiting a continuous downward trend. The Moran's  $I$  of population urbanization and HQ in 2000, 2010, and 2020 globally remained negative but showed an increasing trend, with values of  $-0.189$ ,  $-0.228$ , and  $-0.254$ , respectively, while those of economic urbanization and HQ and land urbanization and HQ also remained negative and exhibited a similar increasing trend. The spatial autocorrelations for both UL and HQ in different dimensions indicated that deserts and plateaus functioned as catchment areas with low UL and low HQ. The CCD between UL and HQ in each county globally ranged from 0 to 0.70, and more than half of the counties globally have achieved basic coordination, with an increasing trend over the study period. Meanwhile, the CCD of land urbanization and HQ in most counties globally was in basic and moderate coordination, indicating a more harmonious relationship between human and land. The CCD between population urbanization and HQ was similar to that of economic urbanization in terms of spatial distribution. There was mostly an extreme and moderate incoordination between population and economic urbanization and HQ. Nevertheless, the CCD of land urbanization in HQ exhibited the greatest degree of

coordination among the three urbanization dimensions during the study period, showing a state of benign coordination. This study provided a global perspective on the interactive coercive relationship between UL and HQ, which was critical for regional sustainability.

**Supplementary Materials:** The following supporting information can be downloaded at <https://www.mdpi.com/article/10.3390/land13111943/s1>, Figure S1: Bivariate LISA cluster maps between global population urbanization and habitat quality from 2000 to 2020; Figure S2: Bivariate LISA cluster maps between global economic urbanization and habitat quality from 2000 to 2020; Figure S3: Bivariate LISA cluster maps between global land urbanization and habitat quality from 2000 to 2020; Figure S4: Spatiotemporal distribution of coupling coordination degree between global population urbanization and habitat quality from 2000 to 2020; Figure S5: Spatiotemporal distribution of coupling coordination degree between global economic urbanization and habitat quality from 2000 to 2020; Figure S6: Spatiotemporal distribution of coupling coordination degree between global land urbanization and habitat quality from 2000 to 2020.

**Author Contributions:** Conceptualization, S.P., and W.C.; methodology, W.L., Y.C., and B.D.; software, W.L., B.D., and S.P.; formal analysis, J.W., Y.Y., and W.C.; data curation, W.L., J.W., Y.Y., and W.C.; writing—original draft preparation, W.L., B.D., S.P., J.W., Y.C., and W.C.; writing—review and editing, W.L., B.D., J.W., Y.Y., S.P., Y.C., and W.C. All authors have read and agreed to the published version of the manuscript.

**Funding:** This research was supported by the China Postdoctoral Science Foundation [Grant No. 2023M733466]. This research was also supported by the Humanities and Social Sciences Research Projects of the Provincial Department of Education [Grant No. 23Q170, No. 22Q160] and the Youth Scientific Research Fund Project of Hubei University of Economics [Grant No. XJYB202309].

**Data Availability Statement:** The original contributions presented in the study are included in the article, further inquiries can be directed to the corresponding authors.

**Acknowledgments:** The authors would like to thank the anonymous reviewers for their constructive comments on improving this paper.

**Conflicts of Interest:** The authors declare no conflicts of interest.

## References

- Mingxing, C.; Yuan, Z.; Shasha, G.; Xinrong, H. Significance, progress and tasks of new-type urbanization research. *Adv. Earth Sci.* **2019**, *34*, 974–983. (In Chinese) [[CrossRef](#)]
- Zhou, L.; Dang, X.; Sun, Q.; Wang, S. Multi-scenario simulation of urban land change in Shanghai by random forest and CA-Markov model. *Sust. Cities Soc.* **2020**, *55*, 102045. [[CrossRef](#)]
- Tang, F.; Wang, L.; Guo, Y.; Fu, M.; Huang, N.; Duan, W.; Luo, M.; Zhang, J.; Li, W.; Song, W. Spatio-temporal variation and coupling coordination relationship between urbanisation and habitat quality in the Grand Canal, China. *Land Use Policy* **2022**, *117*, 106119. [[CrossRef](#)]
- Chen, G.; Li, X.; Liu, X.; Chen, Y.; Liang, X.; Leng, J.; Xu, X.; Liao, W.; Qiu, Y.; Wu, Q.; et al. Global projections of future urban land expansion under shared socioeconomic pathways. *Nat. Commun.* **2020**, *11*, 537. [[CrossRef](#)] [[PubMed](#)]
- Tu, Y.; Chen, B.; Yu, L.; Xin, Q.; Gong, P.; Xu, B. How does urban expansion interact with cropland loss? A comparison of 14 Chinese cities from 1980 to 2015. *Landsc. Ecol.* **2021**, *36*, 243–263. [[CrossRef](#)]
- Ke, X.; van Vliet, J.; Zhou, T.; Verburg, P.H.; Zheng, W.; Liu, X. Direct and indirect loss of natural habitat due to built-up area expansion: A model-based analysis for the city of Wuhan, China. *Land Use Policy* **2018**, *74*, 231–239. [[CrossRef](#)]
- Fang, C.L.; Liu, H.M.; Li, G.D. International progress and evaluation on interactive coupling effects between urbanization and the eco-environment. *J. Geogr. Sci.* **2016**, *26*, 1081–1116. [[CrossRef](#)]
- Xing, L.; Xue, M.G.; Hu, M.S. Dynamic simulation and assessment of the coupling coordination degree of the economy-resource-environment system: Case of Wuhan City in China. *J. Environ. Manag.* **2019**, *230*, 474–487. [[CrossRef](#)]
- Goertz, J.W. Influence of Habitat Quality upon Density of Cotton Rat Populations. *Ecol. Monogr.* **1964**, *34*, 359–381. [[CrossRef](#)]
- Horne, B.V. Density as a misleading indicator of habitat quality. *J. Wildl. Manag.* **1983**, *47*, 893–901. [[CrossRef](#)]
- Kempton, R.A. The structure of species abundance and measurement of diversity. *Biometrics* **1979**, *35*, 307–321. [[CrossRef](#)]
- Tang, F.; Fu, M.C.; Wang, L.; Zhang, P.T. Land-use change in Changli County, China: Predicting its spatio-temporal evolution in habitat quality. *Ecol. Indic.* **2020**, *117*, 106719. [[CrossRef](#)]
- Wei, Q.; Abudurehman, M.; Halike, A.; Yao, K.; Yao, L.; Tang, H.; Tuheti, B. Temporal and spatial variation analysis of habitat quality on the PLUS-InVEST model for Ebinur Lake Basin, China. *Ecol. Indic.* **2022**, *145*, 109632. [[CrossRef](#)]
- Wu, X.L.; Hu, F. Analysis of ecological carrying capacity using a fuzzy comprehensive evaluation method. *Ecol. Indic.* **2020**, *113*, 106243. [[CrossRef](#)]

15. Tang, F.; Fu, M.C.; Wang, L.; Song, W.J.; Yu, J.F.; Wu, Y.B. Dynamic evolution and scenario simulation of habitat quality under the impact of land-use change in the Huaihe River Economic Belt, China. *PLoS ONE* **2021**, *16*, e0249566. [[CrossRef](#)]
16. Terrado, M.; Sabater, S.; Chaplin-Kramer, B.; Mandle, L.; Ziv, G.; Acuña, V. Model development for the assessment of terrestrial and aquatic habitat quality in conservation planning. *Sci. Total Environ.* **2016**, *540*, 63–70. [[CrossRef](#)]
17. He, J.H.; Huang, J.L.; Li, C. The evaluation for the impact of land use change on habitat quality: A joint contribution of cellular automata scenario simulation and habitat quality assessment model. *Ecol. Model.* **2017**, *366*, 58–67. [[CrossRef](#)]
18. Bai, L.; Xiu, C.; Feng, X.; Liu, D. Influence of urbanization on regional habitat quality: A case study of Changchun City. *Habitat Int.* **2019**, *93*, 102042. [[CrossRef](#)]
19. Xie, Z.; Zhang, B.; Shi, Y.; Zhang, X.; Sun, Z. Changes and protections of urban habitat quality in Shanghai of China. *Sci. Rep.* **2023**, *13*, 10976. [[CrossRef](#)]
20. Wei, L.T.; Zhou, L.; Sun, D.; Yuan, B.; Hu, F. Evaluating the impact of urban expansion on the habitat quality and constructing ecological security patterns: A case study of Jiziwan in the Yellow River Basin, China. *Ecol. Indic.* **2022**, *145*, 109544. [[CrossRef](#)]
21. Xu, X.; Xie, Y.; Qi, K.; Luo, Z.; Wang, X. Detecting the response of bird communities and biodiversity to habitat loss and fragmentation due to urbanization. *Sci. Total Environ.* **2018**, *624*, 1561–1576. [[CrossRef](#)] [[PubMed](#)]
22. Younes, I.; Naseem, R.; Sadaf, R.; Shafiq, M.; Zafar, H.; Shahid, A. Monitoring and impact assessment of land use change on environment in Burewala, Punjab through geo-informatics. *Int. J. Econ. Environ. Geol.* **2019**, *8*, 55–62.
23. Zhu, J.; Ding, N.; Li, D.; Sun, W.; Xie, Y.; Wang, X. Spatiotemporal Analysis of the Nonlinear Negative Relationship between Urbanization and Habitat Quality in Metropolitan Areas. *Sustainability* **2020**, *12*, 669. [[CrossRef](#)]
24. Hu, J.; Zhang, J.; Li, Y. Exploring the spatial and temporal driving mechanisms of landscape patterns on habitat quality in a city undergoing rapid urbanization based on GTWR and MGWR: The case of Nanjing, China. *Ecol. Indic.* **2022**, *143*, 109333. [[CrossRef](#)]
25. Zhao, M.; Tian, Y.; Dong, N.; Hu, Y.; Tian, G.; Lei, Y. Spatial and temporal dynamics of habitat quality in response to socioeconomic and landscape patterns in the context of urbanization: A case in Zhengzhou City, China. *Nat. Conserv.* **2022**, *48*, 185–212. [[CrossRef](#)]
26. Luan, Y.; Huang, G.; Zheng, G. Spatiotemporal evolution and prediction of habitat quality in Hohhot City of China based on the InVEST and CA-Markov models. *J. Arid Land* **2023**, *15*, 20–33. [[CrossRef](#)]
27. Chen, L.; Wei, Q.; Fu, Q.; Feng, D. Spatiotemporal Evolution Analysis of Habitat Quality under High-Speed Urbanization: A Case Study of Urban Core Area of China Lin-Gang Free Trade Zone (2002–2019). *Land* **2021**, *10*, 167. [[CrossRef](#)]
28. Zhu, C.; Zhang, X.; Zhou, M.; He, S.; Gan, M.; Yang, L.; Wang, K. Impacts of urbanization and landscape pattern on habitat quality using OLS and GWR models in Hangzhou, China. *Ecol. Indic.* **2020**, *117*, 106654. [[CrossRef](#)]
29. Pan, S.P.; Guo, J.; Ou, M.H. Exploring the coupling and decoupling relationship of urbanization and carbon emissions in China. *Environ. Sci. Pollut. Res.* **2023**, *30*, 96808–96826. [[CrossRef](#)]
30. Wang, S.; Gao, S.; Li, S.; Feng, K. Strategizing the relation between urbanization and air pollution: Empirical evidence from global countries. *J. Clean. Prod.* **2020**, *243*, 118615. [[CrossRef](#)]
31. Wang, Q.; Wang, X.; Li, R. Does urbanization redefine the environmental Kuznets curve? An empirical analysis of 134 Countries. *Sustain. Cities Soc.* **2022**, *76*, 103382. [[CrossRef](#)]
32. Friedmann, J. Four theses in the study of China's urbanization. *Int. J. Urban Reg.* **2006**, *30*, 440–451. [[CrossRef](#)]
33. Peng, J.; Shen, H.; Wu, W.H.; Liu, Y.X.; Wang, Y.L. Net primary productivity (NPP) dynamics and associated urbanization driving forces in metropolitan areas: A case study in Beijing City, China. *Landscape Ecol.* **2016**, *31*, 1077–1092. [[CrossRef](#)]
34. Chen, J.; Gao, M.; Cheng, S.; Hou, W.; Song, M.; Liu, X.; Liu, Y. Global 1 km × 1 km gridded revised real gross domestic product and electricity consumption during 1992–2019 based on calibrated nighttime light data. *Sci. Data* **2022**, *9*, 202. [[CrossRef](#)]
35. Chen, W.; Chi, G. Urbanization and ecosystem services: The multi-scale spatial spillover effects and spatial variations. *Land Use Policy* **2022**, *114*, 105964. [[CrossRef](#)]
36. Yang, M.; Gao, X.; Siddique, K.H.M.; Wu, P.; Zhao, X. Spatiotemporal exploration of ecosystem service, urbanization, and their interactive coercing relationship in the Yellow River Basin over the past 40 years. *Sci. Total Environ.* **2023**, *858*, 159757. [[CrossRef](#)]
37. Zhang, Z.; Peng, J.; Xu, Z.; Wang, X.; Meersmans, J. Ecosystem services supply and demand response to urbanization: A case study of the Pearl River Delta, China. *Ecosyst. Serv.* **2021**, *49*, 101274. [[CrossRef](#)]
38. Peng, Y.; Chen, W.; Pan, S.; Gu, T.; Zeng, J. Identifying the driving forces of global ecosystem services balance, 2000–2020. *J. Clean. Prod.* **2023**, *426*, 139019. [[CrossRef](#)]
39. Zheng, L.; Wang, Y.; Li, J. Quantifying the spatial impact of landscape fragmentation on habitat quality: A multi-temporal dimensional comparison between the Yangtze River Economic Belt and Yellow River Basin of China. *Land Use Policy* **2023**, *125*, 106463. [[CrossRef](#)]
40. Chen, X.; Yu, L.; Cao, Y.; Xu, Y.; Zhao, Z.; Zhuang, Y.; Liu, X.; Du, Z.; Liu, T.; Yang, B.; et al. Habitat quality dynamics in China's first group of national parks in recent four decades: Evidence from land use and land cover changes. *J. Environ. Manag.* **2023**, *325*, 116505. [[CrossRef](#)]
41. Ren, Q.; He, C.; Huang, Q.; Shi, P.; Zhang, D.; Güneralp, B. Impacts of urban expansion on natural habitats in global drylands. *Nat. Sustain.* **2022**, *5*, 869–878. [[CrossRef](#)]
42. Yang, L.; Pan, S.; Chen, W.; Zeng, J.; Xu, H.; Gu, T. Spatially non-stationary response of habitat quality to land use activities in World's protected areas over 20 years. *J. Clean. Prod.* **2023**, *419*, 138245. [[CrossRef](#)]
43. Chen, W.; Gu, T.; Zeng, J. Urbanisation and ecosystem health in the Middle Reaches of the Yangtze River urban agglomerations, China: A U-curve relationship. *J. Environ. Manag.* **2022**, *318*, 115565. [[CrossRef](#)] [[PubMed](#)]



44. Zhou, T.; Chen, W.; Wang, Q.; Li, Y. Urbanisation and ecosystem services in the Taiwan Strait west coast urban agglomeration, China, from the perspective of an interactive coercive relationship. *Ecol. Indic.* **2023**, *146*, 109861. [[CrossRef](#)]
45. Pan, H.; Du, Z.; Wu, Z.; Zhang, H.; Ma, K. Assessing the coupling coordination dynamics between land use intensity and ecosystem services in Shanxi's coalfields, China. *Ecol. Indic.* **2024**, *158*, 111321. [[CrossRef](#)]
46. Tu, D.; Cai, Y.; Liu, M. Coupling coordination analysis and spatiotemporal heterogeneity between ecosystem services and new-type urbanization: A case study of the Yangtze River Economic Belt in China. *Ecol. Indic.* **2023**, *154*, 110535. [[CrossRef](#)]
47. Angel, S.; Parent, J.; Civco, D.L.; Blei, A.; Potere, D. The dimensions of global urban expansion: Estimates and projections for all countries, 2000–2050. *Prog. Plann.* **2011**, *75*, 53–107. [[CrossRef](#)]
48. Seto, K.C.; Güneralp, B.; Hutyrá, L.R. Global forecasts of urban expansion to 2030 and direct impacts on biodiversity and carbon pools. *Proc. Natl. Acad. Sci. USA* **2012**, *109*, 16083–16088. [[CrossRef](#)]
49. Van Vliet, J. Direct and indirect loss of natural area from urban expansion. *Nat. Sustain.* **2019**, *2*, 755–763. [[CrossRef](#)]
50. Duranton, G.; Puga, D. Nursery Cities: Urban Diversity, Process Innovation, and the Life Cycle of Products. *Am. Econ. Rev.* **2001**, *91*, 1454–1477. [[CrossRef](#)]
51. Puga, D. The Magnitude and Causes of Agglomeration Economies. *J. Reg. Sci.* **2010**, *50*, 203–219. [[CrossRef](#)]
52. Barlow, J.; Lennox, G.D.; Ferreira, J.; Berenguer, E.; Lees, A.C.; Nally, R.M.; Thomson, J.R.; Ferraz, S.F.D.B.; Louzada, J.; Oliveira, V.H.F.; et al. Anthropogenic disturbance in tropical forests can double biodiversity loss from deforestation. *Nature* **2016**, *535*, 144–147. [[CrossRef](#)] [[PubMed](#)]
53. Armenteras, D.; Schneider, L.; Gast, F. Deforestation and forest degradation due to gold mining in the Peruvian Amazon: A 34-year perspective. *Remote Sens. Environ.* **2019**, *233*, 1903. [[CrossRef](#)]
54. Sharma, R.; Rimal, B.; Stork, N.; Baral, H.; Dhakal, M. Spatial assessment of the potential impact of infrastructure development on biodiversity conservation in Lowland Nepal. *ISPRS Int. J. Geo-Inf.* **2018**, *7*, 365. [[CrossRef](#)]
55. Geist, H.J.; Lambin, E.F. Proximate causes and underlying driving forces of tropical deforestation. *Bioscience* **2002**, *52*, 143–150. [[CrossRef](#)]
56. Curtis, P.G.; Slay, C.M.; Harris, N.L.; Tyukavina, A.; Hansen, M.C. Classifying drivers of global forest loss. *Science* **2018**, *361*, 1108–1111. [[CrossRef](#)]
57. Terra dos Santos, L.C.; Frimaio, A.; Giannetti, B.F.; Agostinho, F.; Liu, G.; Almeida, C.M. Integrating Environmental, Social, and Economic Dimensions to Monitor Sustainability in the G20 Countries. *Sustainability* **2023**, *15*, 6502. [[CrossRef](#)]
58. Mohanty, M. Sustainable Urban Planning and Making Sustainable Cities. In *Sustainable Cities and Communities. Encyclopedia of the UN Sustainable Development Goals*; Leal Filho, W., Azul, A., Brandli, L., Özuyar, P., Wall, T., Eds.; Springer: Cham, Switzerland, 2020; pp. 1–12. [[CrossRef](#)]
59. Bai, X.M.; Shi, P.J.; Liu, Y.S. Society: Realizing China's urban dream. *Nature* **2014**, *509*, 158–160. [[CrossRef](#)]
60. Sahana, M.; Hong, H.; Sajjad, H. Analyzing urban spatial patterns and trend of urban growth using urban sprawl matrix: A study on Kolkata urban agglomeration, India. *Sci. Total Environ.* **2018**, *628–629*, 1557–1566. [[CrossRef](#)]
61. Fang, C.; Li, G.; Wang, S. Changing and Differentiated Urban Landscape in China: Spatiotemporal Patterns and Driving Forces. *Environ. Sci. Technol.* **2016**, *50*, 2217–2227. [[CrossRef](#)]
62. Chen, H.; Jia, B.; Lau, S.S.Y. Sustainable urban form for Chinese compact cities: Challenges of a rapid urbanized economy. *Habitat Int.* **2008**, *32*, 28–40. [[CrossRef](#)]
63. Cortinovis, C.; Haase, D.; Zanon, B.; Geneletti, D. Is urban spatial development on the right track? Comparing strategies and trends in the European Union. *Landsc. Urban Plan.* **2019**, *181*, 22–37. [[CrossRef](#)]
64. Boyle, R.; Mohamed, R. State growth management, smart growth and urban containment: A review of the US and a study of the heartland. *J. Environ. Plann. Man.* **2007**, *50*, 677–697. [[CrossRef](#)]
65. Bunker, R. How Is the compact city faring in Australia? *Plan. Pract. Res.* **2014**, *29*, 449–460. [[CrossRef](#)]
66. Seto, K.C.; Kaufmann, R.K.; Woodcock, C.E. Landsat reveals China's farmland reserves, but they're vanishing fast. *Nature* **2000**, *406*, 121. [[CrossRef](#)]
67. Grimm, N.B.; Faeth, S.H.; Golubiewski, N.E.; Redman, C.L.; Wu, J.; Bai, X.; Briggs, J.M. Global change and the ecology of cities. *Science* **2008**, *319*, 756–760. [[CrossRef](#)]
68. Montesino Pouzols, F.; Toivonen, T.; Di Minin, E.; Kukkala, A.S.; Kullberg, P.; Kuusterä, J.; Lehtomäki, J.; Tenkanen, H.; Verburg, P.H.; Moilanen, A. Global protected area expansion is compromised by projected land-use and parochialism. *Nature* **2014**, *516*, 383–386. [[CrossRef](#)]
69. Michetti, M.; Zampieri, M. Climate–human–land interactions: A review of major modelling approaches. *Land* **2014**, *3*, 793–833. [[CrossRef](#)]
70. Liu, J.; Liu, W.; Allechy, F.B.; Zheng, Z.; Liu, R.; Kouadio, K.L. Machine learning-based techniques for land subsidence simulation in an urban area. *J. Environ. Manag.* **2024**, *352*, 120078. [[CrossRef](#)]
71. Westerink, J.; Haase, D.; Bauer, A.; Ravetz, J.; Jarrige, F.; Aalbers, C.B. Dealing with sustainability trade-offs of the compact city in peri-urban planning across European city regions. *Eur. Plan. Stud.* **2013**, *21*, 473–497. [[CrossRef](#)]

**Disclaimer/Publisher's Note:** The statements, opinions and data contained in all publications are solely those of the individual author(s) and contributor(s) and not of MDPI and/or the editor(s). MDPI and/or the editor(s) disclaim responsibility for any injury to people or property resulting from any ideas, methods, instructions or products referred to in the content.